



Novel chromophores with excellent electro-optic activity based on double-donor chromophores by optimizing thiophene bridges



Yuhui Yang^{a, b}, Shuhui Bo^{a, **}, Haoran Wang^{a, b}, Fenggang Liu^{a, b}, Jialei Liu^a, Ling Qiu^a, Zhen Zhen^a, Xinhou Liu^{a, *}

^a Key Laboratory of Photochemical Conversion and Optoelectronic Materials, Technical Institute of Physics and Chemistry, Chinese Academy of Sciences, Beijing 100190, PR China

^b University of Chinese Academy of Sciences, Beijing 100043, PR China

ARTICLE INFO

Article history:

Received 31 May 2015

Received in revised form

10 June 2015

Accepted 13 June 2015

Available online 23 June 2015

Keywords:

Double-donor chromophores

Electro-optic

Isolation group

Poled film

NLO

DFT

ABSTRACT

Three novel nonlinear optical chromophores based on the same bis(*N,N*-diethyl)aniline donor have been synthesized and systematically characterized. These chromophores showed good thermal stability and chromophore y1 showed the best thermal stability of 249 °C. Besides, compared with the chromophore (y1) without the substituted group, chromophores y2 and y3 show better intramolecular charge-transfer absorption. Most importantly, the high molecular hyperpolarizability of these chromophores can be effectively translated into large electro-optic coefficients. The electro-optic coefficient of poled films containing 25% wt of chromophores y1–y3 doped in amorphous polycarbonate afforded values of 149, 138 and 157 pm/V at 1310 nm for chromophores y1–y3 respectively. These results indicated that the double donors of bis(*N,N*-diethyl)aniline unit can efficiently improve the electron-donating ability and the special structure can reduce intermolecular electrostatic interactions, thus enhancing the macroscopic electro-optic activity. These properties, together with good solubility, suggest the potential use of these chromophores as advanced materials.

© 2015 Elsevier Ltd. All rights reserved.

1. Introduction

Polymeric electro-optic (EO) materials with nonlinear optical (NLO) chromophores have shown commercial potential as active media in high-speed broadband waveguides for optical switches, optical sensors, and information processors [1–5]. In the past two decades, the NLO materials have continuously drawn great interest and have stimulated a research boom for materials with large EO activities, both at molecular level (β) and as processed materials (r_{33}). Considerable progress has been made on developing organic and polymeric electro-optic (EO) materials for applications in high-speed and broadband information technology [2,5–7]. However, one major obstacle that hinders the rapid development of this technology is the lack of an effective mechanism to translate high-molecular nonlinearities (β) into large macroscopic EO activities (r_{33}) [8,9]. Efficient translation of large β chromophores into

thermally and chemically stable materials with macroscopic EO responses can be achieved by careful modification of the molecular structure of chromophores and host polymers under mild electric-field poling [10–12]. Thus, chromophores with large β and weak inter-molecular electrostatic interaction, as the decisive factor, must be designed and prepared.

In general, dipolar NLO chromophores used in polymeric EO materials consist of electron-donor and electron-acceptor groups interacting through a conjugated bridge. In such molecules, the donor and acceptor substituents provide the requisite ground-state charge asymmetry, whereas the π -conjugation bridge provides a pathway for the ultrafast redistribution of electric charges under an applied external electric field [4,13,14]. The traditional chromophore moieties have a rod-like structure, which leads to strong inter-molecular dipole–dipole interactions in the polymeric matrix and makes the poling-induced noncentrosymmetric alignment of the chromophores a daunting task. For this reason, many efforts have been carried out to design and synthesize novel NLO chromophores, seeking to engineer NLO molecules both microscopically (β) and macroscopically (r_{33}). On one hand, it has been well established that large β values of the chromophores can be

* Corresponding author. Tel.: +86 01 82543528; fax: +86 01 62554670.

** Corresponding author. Tel.: +86 01 82543528; fax: +86 01 62554670.

E-mail addresses: boshuhui@mail.ipc.ac.cn (S. Bo), xinhouliu@foxmail.com (X. Liu).

achieved by careful modification of the strength of donor and acceptor moieties, as well as the nature of the π -conjugated spacer [15,16]. Until now, NLO chromophores containing thiophene based bridges have been widely used [17,18]. Further modification was also widely studied to achieve excellent and better performance [19–22]. On the other hand, controlling the shape of the chromophore was proven to be an efficient approach for minimizing intermolecular dipole–dipole interaction and enhancing the poling efficiency [23]. So modifying the thiophene bridge may be one of a reasonable way to achieve excellent and better performance.

Based on above point, as well as our previous work on the “double-donor chromophore” [5,9,24], we designed and synthesized three new double donor chromophores **y1**, **y2**, and **y3**. In our previous work, it has been shown from both theoretical and experimental analysis that the linear and nonlinear optical properties of double-donor chromophores are excellent. It also can translate the high β values of the chromophores to large macroscopic optical nonlinearities (r_{33}) values. The double donors with two *N,N*-diethylaniline can improve the electron-donating ability thus enhance the optical nonlinearity. The one of the *N,N*-diethylaniline unit can act as both the additional donor and the isolation group (IG). On the other hand, the double benzene rings with an appropriate angle make the special structure different from the general NLO chromophores and can decrease the intermolecular electrostatic interactions so enhance the macroscopic EO activity. However, to our regret, the solubility of double-donor chromophore is not so excellent and limited its application, which encourage us to optimize double-donor chromophore. In this paper, a new synthetic methodology of attaching two different substituents onto the π -conjugation bridge of NLO chromophore was developed to obtain two new NLO chromophores. The motivation is to improve the solubility as well as the EO activities of guest-host EO materials by a simple bridge-modifying method for NLO chromophores. These modified chromophores showed great solubility in common organic solvents, better thermal stability (with their onset decomposition temperatures all above 220 °C), good compatibility with polymers, and large EO activity in the poled films. ^1H NMR and ^{13}C NMR analysis were carried out to demonstrate the preparation of these chromophores. Thermal stability, photophysical properties and DFT calculations of these chromophores were systematically studied. Furthermore, the macroscopic EO activity (r_{33}) of these chromophores in amorphous polycarbonate were also analysed [Chart 1](#).

2. Experiments

2.1. Materials and instrumentation

^1H NMR spectra were determined by an Advance Bruker 400 (400 MHz) NMR spectrometer (tetramethylsilane as internal reference). The MS spectra were obtained on MALDI-TOF (Matrix Assisted Laser Desorption/Ionization of Flight) on BIFLEXIII (Broker Inc.) spectrometer. The UV–Vis spectra were performed on Cary 5000 photo spectrometer. The TGA was determined by TA5000-

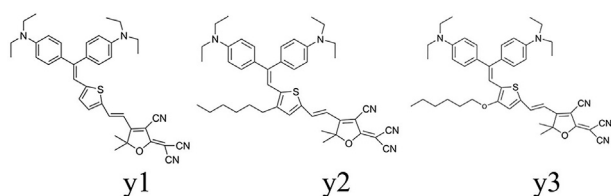


Chart 1. Structure of chromophore **y1–y3**.

2950TGA (TA Co) with a heating rate of 10 °C/min under the protection of nitrogen. Cyclic voltammetry (CV) experiments were performed on a CHI660D electrochemical workstation by a cyclic voltammetry (CV) technique in CH_3CN solution, using Pt disk electrode and a Pt wire as the working and counter electrodes, respectively, and a saturated Ag/AgCl electrode as the reference electrode in the presence of 0.1 M *n*-tetrabutylammoniumperchlorate as the supporting electrolyte. The ferrocene/ferrocenium (Fc/Fc⁺) couple was used as an internal reference. All chemicals, commercially available, are used without further purification unless stated. The DMF, POCl_3 and THF were freshly distilled prior to its use. The 2-dicyanomethylene-3-cyano-4-methyl-2,5-dihydrofuran (TCF) acceptor was prepared according to the literature [25].

2.2. Synthesis

2.2.1. Synthesis of chromophore **y1**

Chromophore **y1** was synthesized according to the literature [24].

2.2.2. Synthesis of compound **2b**

Dry DMF (3 mL) was dropwise added to 3 mL of phosphorus oxychloride (0.0327 mol) maintained at 0 °C. After the solution was stirred for 30 min, compound **1b** (4.60 g, 0.0274 mol) was added to the above Vilsmeier reagent, and the mixture was heated to 90 °C for an additional 2 h. After cooling, the clear red solution was added dropwise to NaHCO_3 (aq) with stirring, and the resulting mixture was allowed to stand for 2 h and extracted with CH_2Cl_2 (20 mL \times 3). The combined extracts were washed with water and dried over MgSO_4 . After filtration and removal of the solvent under vacuum, the crude product was purified by column chromatography to give a red liquid product (87%).

^1H NMR (400 MHz, CDCl_3) δ 9.99 (s, 1H), 7.58 (d, $J = 5.0$ Hz, 1H), 6.96 (d, $J = 5.0$ Hz, 1H), 2.98–2.62 (m, 2H), 1.73–1.53 (m, 2H), 1.37–1.12 (m, 6H), 0.83 (m, 3H).

^{13}C NMR (100 MHz, CDCl_3) δ 182.18, 152.90, 137.71, 134.42, 130.80, 31.65, 31.61, 31.45, 30.42, 30.18, 29.00, 28.53, 22.63, 14.09.

MS (EI): m/z calcd for $\text{C}_{11}\text{H}_{16}\text{OS}$: 196.09; found: 196.31.

2.2.3. Synthesis of compound **3b**

To a suspension of diethyl bis(4-(diethylamino) phenyl) methylphosphonate (1.5 g, 3.36 mmol), and **2b** (588 mg, 3 mmol) in 20 mL dry THF and NaH (0.36 g, 15 mmol) were added and the mixture turned yellow. The mixture was stirred at room temperature for 24 h. Saturated NH_4Cl was added and the resulting mixture was extracted with EtOAc (20 mL \times 3). The combined extracts were washed with water and dried over MgSO_4 . After filtration and removal of the solvent under vacuum, the crude product was purified by column chromatography to give a yellow product (0.66 g, 45%).

^1H NMR (400 MHz, Acetone) δ 7.07–7.01 (m, 2H), 6.90 (s, 1H), 6.87–6.82 (m, 3H, overlap), 6.63 (d, $J = 3.8$ Hz, 1H), 6.62 (d, $J = 8.8$ Hz, 2H), 6.50 (d, $J = 8.8$, 2H), 3.29 (m, 8H), 2.63–2.54 (m, 2H), 1.49 (m, 2H), 1.31–1.20 (m, 6H), 1.04 (m, 12H), 0.75 (m, 3H).

MALDI-TOF: m/z calcd for $\text{C}_{32}\text{H}_{44}\text{N}_2\text{S}$: 488.32 [M]⁺; found: 488.09.

2.2.4. Synthesis of compound **4b**

To a solution of **3b** (0.98 g, 2.0 mmol) in dry THF (20 mL) was added a 2.4 M solution of *n*-BuLi in hexane (1.3 mL, 3.0 mmol) dropwise at -78 °C under N_2 . After this mixture was stirred at this temperature for 1 h, and the dry DMF (0.20 mL, 2.4 mmol) was introduced. The resulting solution was stirred for another 1 h at -78 °C and then allowed to warm up to room temperature. The

reaction was quenched by water. THF was removed by evaporation. The residue was extracted with CH_2Cl_2 (3×30 mL). The organic layer was dried (MgSO_4) and concentrated in vacuo. The residue was purified by column chromatography on silica gel (hexane/acetone, v/v, 10/1) to obtain a red liquid (0.85 g, 82%).

^1H NMR (400 MHz, CDCl_3) δ 9.69 (s, 1H), 7.44 (s, 1H), 7.31–7.25 (m, 3H, overlap), 7.07 (d, $J = 8.6$ Hz, 2H), 7.01 (s, 1H), 6.74 (d, $J = 8.6$ Hz, 2H), 6.64 (d, $J = 8.7$ Hz, 2H), 3.43 (m, 8H), 2.72 (m, 2H), 1.67 (m, 2H), 1.39 (m, 6H), 1.23 (m, 12H), 0.97–0.91 (m, 3H).

^{13}C NMR (100 MHz, CDCl_3) δ 182.24, 148.26, 148.04, 147.79, 146.37, 141.88, 139.03, 137.59, 131.41, 129.60, 129.12, 125.10, 44.43, 44.36, 31.73, 30.55, 29.14, 28.91, 22.67, 14.14, 12.67, 12.65.

MALDI-TOF: m/z calcd for $\text{C}_{33}\text{H}_{44}\text{N}_2\text{OS}$: 516.32 $[\text{M}]^+$; found:516.73.

2.2.5. Synthesis of chromophore **y2**

A mixture of aldehydic bridge **4b** (0.516 g, 1 mmol) and acceptor **5** (0.24 g, 1.2 mmol) in ethanol (20 mL) with a catalytic amount of piperidine and stirred at 78°C for 3 h. After removal of the solvent, the residue was purified by column chromatography on silica gel (hexane/ethyl acetate, v/v, 5:1), a dark solid was obtained (0.24 g, 35%).

^1H NMR (400 MHz, Acetone) δ 7.94 (d, $J = 15.7$ Hz, 1H), 7.50 (s, 1H), 7.29 (d, $J = 9.0$ Hz, 2H), 7.19 (s, 1H), 7.01 (d, $J = 8.8$ Hz, 2H), 6.86 (d, $J = 8.8$ Hz, 2H), 6.70 (d, $J = 9.0$ Hz, 2H), 6.41 (d, $J = 15.7$ Hz, 1H), 3.47 (m, 8H), 2.80–2.79 (m, 2H), 1.78 (s, 6H), 1.73–1.67 (m, 2H), 1.48–1.29 (m, 6H), 1.21 (m, 12H), 0.90 (m, 3H).

^{13}C NMR (100 MHz, Acetone) δ 176.58, 173.83, 148.64, 148.49, 148.32, 147.83, 143.98, 140.17, 138.19, 137.30, 131.26, 129.24, 128.78, 124.61, 113.15, 112.64, 112.26, 111.96, 111.19, 110.85, 110.68, 97.59, 95.52, 44.20, 44.07, 31.51, 30.38, 25.52, 22.51, 22.40, 13.46, 12.05, 12.04.

MALDI-TOF: m/z calcd for $\text{C}_{44}\text{H}_{51}\text{N}_5\text{OS}$: 697.38 $[\text{M}]^+$; found:697.93.

HRMS (ESI) ($\text{M} + \text{H}^+$): calcd, 698.3893; found, 698.3874.

2.2.6. Synthesis of compound **1c**

Compound **1c** was synthesis according to the report [26].

^1H NMR (400 MHz, Acetone) δ 7.13 (dd, $J = 5.2, 3.1$ Hz, 1H), 6.72 (dd, $J = 5.2, 1.5$ Hz, 1H), 6.19 (dd, $J = 3.1, 1.5$ Hz, 1H), 3.91 (m, 2H), 1.79–1.69 (m, 2H), 1.42 (m, 2H), 1.36–1.28 (m, 4H), 0.91–0.84 (m, 3H).

MS (EI): m/z calcd for $\text{C}_{10}\text{H}_{16}\text{OS}$: 184.09; found: 184.51.

2.2.7. Synthesis of compound **2c**

In a similar manner described above, **2c** was synthesized from **1c** as a red liquid (72%).

^1H NMR (400 MHz, CDCl_3) δ 10.02 (s, 1H), 7.63 (d, $J = 5.4$ Hz, 1H), 6.85 (d, $J = 5.4$ Hz, 1H), 4.16 (t, $J = 6.5$ Hz, 2H), 1.93–1.74 (m, 4H), 1.40–1.20 (m, 4H), 0.95–0.85 (m, 3H).

MS (EI): m/z calcd for $\text{C}_{11}\text{H}_{16}\text{O}_2\text{S}$: 212.09; found: 212.43.

2.2.8. Synthesis of compound **3c**

In a similar manner described above, **3c** was synthesized from **2c** as a yellow liquid (40%).

^1H NMR (400 MHz, CDCl_3) δ 7.22 (d, $J = 8.8$ Hz, 2H), 7.08 (d, $J = 8.5$ Hz, 2H), 6.80 (d, $J = 5.5$ Hz, 1H), 6.74 (d, $J = 8.5$ Hz, 2H), 6.67 (d, $J = 5.5$ Hz, 1H), 6.62–6.56 (d, $J = 8.8$ Hz, 2H), 4.01 (m, 2H), 3.45–3.30 (m, 8H), 1.96 (m, 2H), 1.76–1.27 (m, 6H), 1.22 (m, 12H), 0.89–0.84 (m, 3H).

MALDI-TOF: m/z calcd for $\text{C}_{32}\text{H}_{44}\text{N}_2\text{OS}$: 504.32 $[\text{M}]^+$; found:504.01.

2.2.9. Synthesis of compound **4c**

In a similar manner described above, **4c** was synthesized from **3c** as a red liquid (78%).

^1H NMR (400 MHz, Acetone) δ 9.55 (s, 1H), 7.49 (s, 1H), 7.14 (s, 1H), 7.08 (d, $J = 8.9$ Hz, 2H), 6.91 (d, $J = 8.6$ Hz, 2H), 6.73 (d, $J = 8.6$ Hz, 2H), 6.56 (d, $J = 8.9$ Hz, 2H), 4.07 (q, $J = 6.7$ Hz, 2H), 3.43–3.26 (m, 8H), 1.96 (m, 2H), 1.74–1.23 (m, 6H), 1.12 (m, 6H), 1.05 (m, 6H), 0.88–0.71 (m, 3H).

^{13}C NMR (100 MHz, Acetone) δ 181.76, 155.51, 148.12, 147.71, 143.97, 136.99, 132.33, 131.00, 129.25, 128.52, 125.45, 123.66, 112.32, 111.41, 111.16, 71.56, 44.03, 31.47, 25.65, 22.48, 13.50, 12.11, 12.03.

MALDI-TOF: m/z calcd for $\text{C}_{33}\text{H}_{44}\text{N}_2\text{O}_2\text{S}$: 532.31 $[\text{M}]^+$; found:532.78.

2.2.10. Synthesis of chromophore **y3**

In a similar manner described above, chromophore **y3** was synthesized from **4c** as a dark solid (38%).

^1H NMR (400 MHz, Acetone) δ 7.73 (d, $J = 15.6$ Hz, 1H), 7.37 (s, 1H), 7.18 (s, 1H), 7.12 (d, $J = 8.9$ Hz, 2H), 6.88 (d, $J = 8.6$ Hz, 2H), 6.74 (d, $J = 8.6$ Hz, 2H), 6.56 (d, $J = 8.9$ Hz, 2H), 6.34 (d, $J = 15.6$ Hz, 1H), 4.04 (t, $J = 6.4$ Hz, 2H), 3.41–3.25 (m, 8H), 1.76–1.67 (m, 2H), 1.65 (s, 6H), 1.41 (m, 2H), 1.26 (m, 2H), 1.14 (m, 2H), 1.14–1.07 (m, 6H), 1.04 (m, 6H), 0.83–0.75 (m, 3H).

^{13}C NMR (100 MHz, Acetone) δ 176.47, 172.97, 157.46, 148.66, 148.29, 146.32, 139.56, 135.20, 135.09, 131.02, 128.98, 128.77, 124.91, 121.72, 112.69, 112.47, 111.97, 111.62, 111.32, 111.01, 110.01, 101.41, 97.29, 94.64, 71.66, 44.20, 44.06, 31.36, 25.53, 22.36, 13.33, 12.04.

MALDI-TOF: m/z calcd for $\text{C}_{44}\text{H}_{51}\text{N}_5\text{O}_2\text{S}$: 713.38 $[\text{M}]^+$; found:713.02.

HRMS (ESI) ($\text{M} + \text{H}^+$): calcd, 714.3842; found, 714.3835.

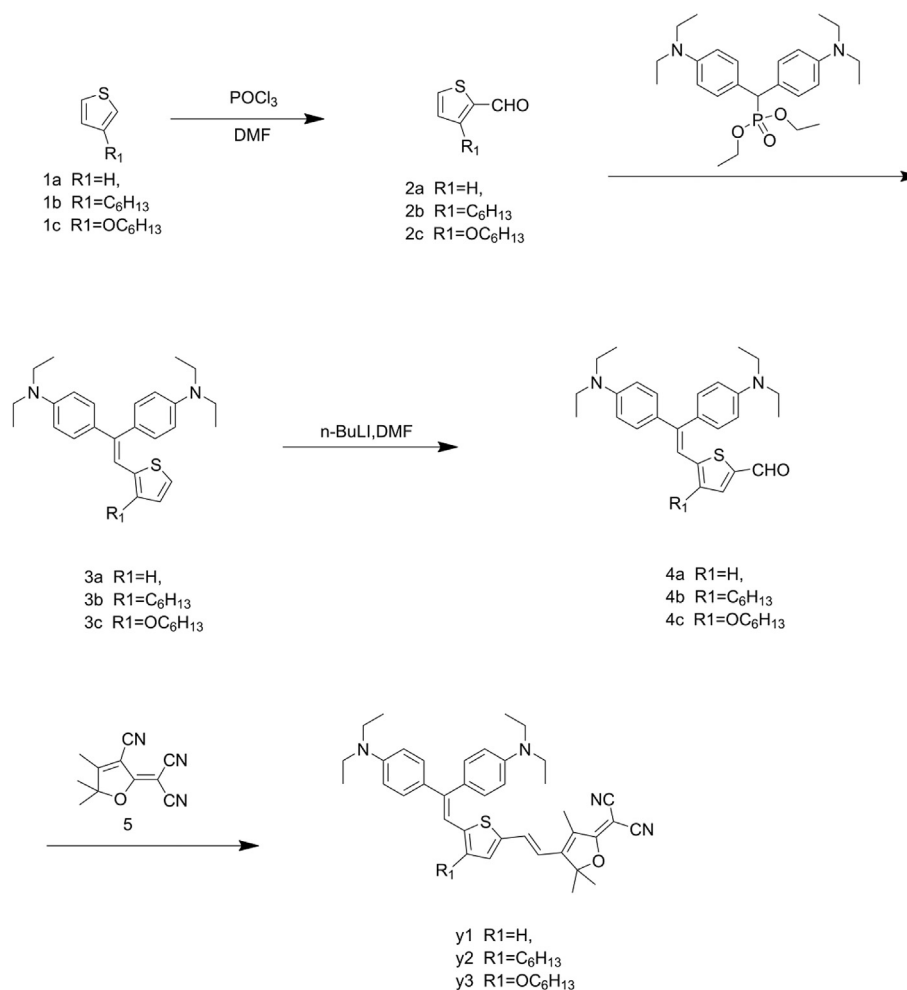
3. Results and discussion

3.1. Synthesis and characterization of chromophores

The synthesis of chromophores **y1**, **y2**, and **y3** are depicted in [Scheme 1](#). These NLO chromophores were designed having same strong electron acceptor (TCF) and the same electron donor bis(*N,N*-diethyl)aniline group, but have different substituent groups on the thiophene π -conjugation. Chromophores **y1**, **y2**, and **y3** were prepared starting from the phosphonate which was prepared using a procedure described in the literature [24,27]. Reacting phosphonate with different aldehyde (**2a–2c**) using sodium hydride as base under a Horner–Emmons reaction condition afforded alkene **3a–3c** exclusively. Lithiation the alkene **3** with *n*-butyl lithium followed by the addition of DMF yielded the corresponding aldehyde **4a–4c**. The target chromophores **y1** (with no substituent), **y2** (with hexyl group) and **y3** (with hexyloxy group) on the bridge thiophene ring were successfully obtained by condensing aldehydes **4a–4c** with acceptor **5** (TCF) in ethanol with the presence of a catalytic amount of piperidine.

3.2. Thermal analysis

The NLO chromophores must be thermally stable enough to withstand encountered high temperatures ($>200^\circ\text{C}$) in electric field poling and subsequent processing of chromophore/polymer materials. Thermal properties of these chromophores were measured by Thermogravimetric Analysis (TGA) with a heating rate of $10^\circ\text{C min}^{-1}$ under nitrogen. [Fig. 1](#) shows the thermogravimetric analysis of chromophores **y1**, **y2**, and **y3**. All of the chromophores exhibited good thermal-stabilities and their decomposition temperatures (T_d) were above 220°C as summarized in [Table 1](#). The excellent thermal stability of these chromophores makes them suitable for practical device fabrication and EO device preparation.



Scheme 1. Synthesis of chromophore y1–y3.

3.3. Optical properties

In order to explore the effect of different substituted groups of the π -conjugation bridge on the intramolecular charge transfer

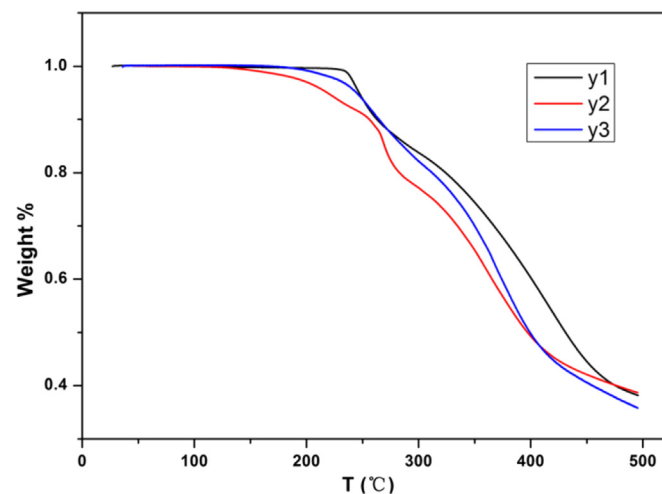


Fig. 1. TGA curves of chromophores y1–y3 with a heating rate of 10 °C min⁻¹ in a nitrogen atmosphere.

(ICT) absorption properties, UV–Vis absorption spectra of three chromophores ($c = 1 \times 10^{-5}$ mol/L) were recorded in a series of solvents with different dielectric constants (Fig. 2). The spectrum data are summarized in Table 1. The synthesized chromophores exhibited a similar π – π^* intramolecular charge-transfer (ICT) absorption band in the visible region. As shown in Fig. 2, in both non-polar and polar solvents such as 1,4-dioxane and CHCl₃, these chromophores exhibited a similar π – π^* intramolecular charge-transfer (ICT) absorption band with a continuous red-shift of the maximum absorption (λ_{\max}) from y1 to y3. Chromophore y3 showed the maximum absorption (λ_{\max}) of 803 nm in CHCl₃. This value is exceptionally large compared to the chromophore y1 (λ_{\max} of 725 nm in CHCl₃) with same donor and the same acceptor but no substituent on thiophene bridge. With a hexyloxy on the thiophene bridge, the λ_{\max} of y3 red shifted by 78 nm. However, with a hexyloxy on the thiophene bridge, the chromophore y2 is only red shifted by 11 nm to 736 nm compared to chromophore y1, which indicated that the hexyloxy group on the thiophene bridge can act as an additional donor and shifted the ICT absorption band of the chromophore to the much lower energy. Besides, the solvatochromic behaviour was also an important aspect to investigate the polarity of chromophores. As shown in Fig. 2, the peak wavelength of chromophores y3 showed a bathochromic shift of 101 nm from dioxane to chloroform, displaying a much larger solvatochromism compared with the chromophore y2 (66 nm) and chromophore y1 (71 nm in Table 1). The resulting spectrum data

Table 1

Summary of thermal and optical properties and EO coefficients of chromophores y1–y3.

Chromophore	T_d^a (°C)	λ_{\max}^b (nm)	λ_{\max}^c (nm)	$\Delta\lambda^d$ (nm)	r_{33}^e (pm/V)
y1	249	725	654	71	149
y2	224	736	670	66	138
y3	246	803	702	101	157

^a T_d was determined by an onset point, and measured by TGA under nitrogen at a heating rate of 10 °C/min.

^b λ_{\max} was measured in CHCl_3 .

^c λ_{\max} was measured in dioxane.

^d $\Delta\lambda = \lambda_{\max}^b - \lambda_{\max}^c$.

^e r_{33} values were measured at the wavelength of 1310 nm.

indicated that the chromophores y3 were more easily polarizable than chromophore y1 and y2.

3.4. Theoretical calculations

For further comparison, we have performed the quantum chemical calculations within a framework of GAUSSIAN 03 using the split valence B3LYP functional with 6-311 G** (d, p) basis set to understand the ground-state polarization of these chromophores with different bridges [28–30]. The data obtained from DFT calculations are summarized in Table 2.

The frontier molecular orbitals are often used to characterize the chemical reactivity and kinetic stability of a molecule and to obtain qualitative information about the optical and electrical properties of molecules. [30–32]. Besides, the HOMO-LUMO energy gap is also used to understand the charge transfer interaction occurring in a chromophore molecule [32–34]. In the case of these chromophores, Fig. 3 represents the frontier molecular orbitals of chromophores y1–y3. According to Fig. 3, it is clear that the electronic distribution of the HOMO is delocalized over the thiophene linkage and benzene ring, whereas the LUMO is mainly constituted by the acceptor moieties [32].

The HOMO and LUMO energy were calculated by DFT calculations as shown in Table 2. The energy gap between the HOMO and LUMO energy for chromophores y1–y3 were 2.05 eV, 1.95 eV and 1.81 eV respectively. The HOMO-LUMO gap was the lowest for chromophore y3 (1.81 eV) and highest for chromophore y1 (2.05 eV). As reported [32], the optical gap is lower and the charge-transfer (ICT) ability is greater, thus improving the nonlinearity. As a result, chromophore y2 and y3 showed the lower optical gap than chromophore y1, so it may indicate that chromophore y2 and y3 can exhibit better ICT and NLO properties than chromophore y1. This result corresponds with the UV–Vis results.

Further, the theoretical microscopic Zero-frequency (static) molecular first hyperpolarizability (β) was calculated by Gaussian 03. As the reference reported earlier, the β has been calculated at the 6-311 g** (d, p) level in vacuum [35]. From this, the scalar quantity of β can be computed from the x, y, and z components according to the following equation:

$$\beta = (\beta_x^2 + \beta_y^2 + \beta_z^2)^{1/2} \quad (1)$$

where $\beta_i = \beta_{iii} + \frac{1}{3} \sum_{i \neq j} (\beta_{ijj} + \beta_{jji} + \beta_{jii})$, $i, j \in (x, y, z)$.

The data obtained from DFT calculations were summarized in Table 2. There was no obvious change of the β values of these chromophores y1–y3 ($684\text{--}713 \times 10^{-30}$ esu), which illustrated that the substituent group on the thiophene bridge had little influence on their main conjugated structures under the simulated condition.

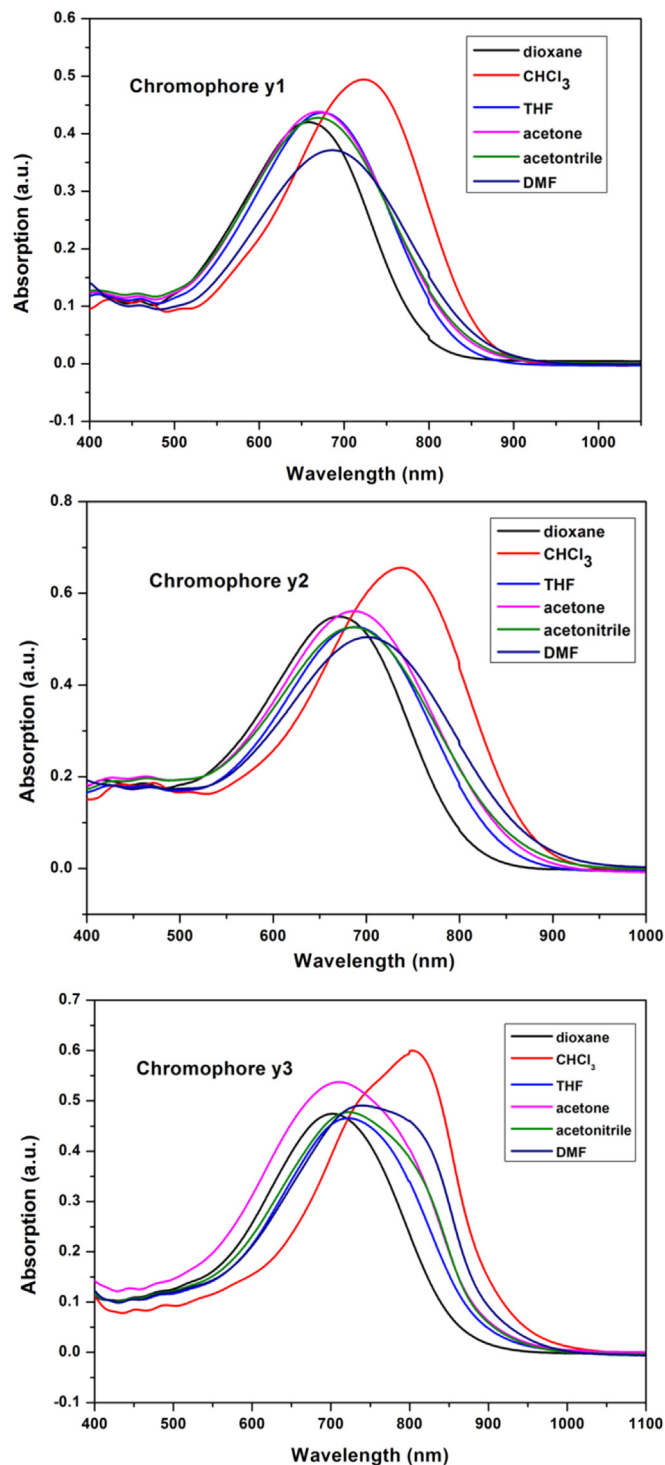


Fig. 2. UV–Vis absorption spectra in different solvents of chromophore y1–y3 ($c = 1 \times 10^{-5}$ mol L^{-1}).

3.5. Electrochemical properties

To determine the redox properties of these chromophores, cyclic voltammetry (CV) experiments were performed on a CHI660D electrochemical workstation by a cyclic voltammetry (CV) technique. As shown in Fig. 4, chromophores y1, y2 and y3 all exhibited one quasi reversible oxidative wave with a half-wave potential, $E_{1/2} = 0.5 (E_{\text{ox}} + E_{\text{red}})$, at about 0.55, 0.51 and 0.43 V respectively.

Table 2
Data from DFT calculations.

Chromophores	$E_{\text{HOMO}}/\text{eV}$	$E_{\text{LUMO}}/\text{eV}$	$\Delta E^{\text{a}}/\text{eV}$	$\Delta E^{\text{b}}/\text{eV}$	$\beta_{\text{max}}^{\text{c}}/10^{-30}$ esu
y1	-5.04	-2.99	2.05	1.12	713
y2	-5.13	-3.18	1.95	1.04	684
y3	-4.98	-3.17	1.81	0.95	686

$\Delta E = E_{\text{LUMO}} - E_{\text{HOMO}}$.

^a Results was calculated by DFT.

^b Results was from cyclic voltammetry experiment.

^c β values were calculated using gaussian03 at B3LYP/6-311 G** (d, p) level and the direction of the maximum value is directed along the charge transfer axis of the chromophores.

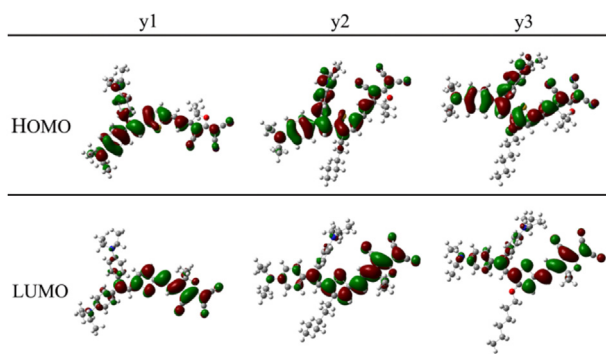


Fig. 3. The frontier molecular orbitals of chromophores y1–y3.

Meanwhile, these chromophores had an irreversible reduction wave corresponding to the acceptor moieties at $E_{\text{red}} = -0.58, -0.53$ and -0.52 V (vs. Ag/AgCl). It showed an energy gap (ΔE) value of 1.12, 1.04 and 0.95 eV for chromophores y1, y2 and y3 respectively. The HOMO and LUMO levels of these new chromophores were calculated from their corresponding oxidation and reduction potentials. The HOMO levels of y1, y2 and y3 were estimated to be $-4.95, -4.91$ and -4.83 eV respectively. In the meantime, the corresponding LUMO level of y1–y3 only showed slight changes at $-3.82, -3.87$ and -3.88 eV, respectively. This result corresponded with the conclusion of UV–Vis spectra analysis and the DFT results.

3.6. Electric field poling and EO property measurements

For application, the large hyperpolarizability (β) has to be translated into a large EO coefficient (r_{33}). To study EO property

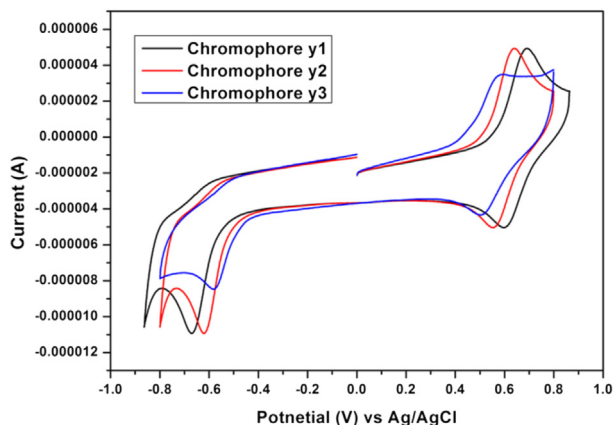


Fig. 4. Cyclic voltammograms of chromophore y1–y3.

Table 3
Summary of EO coefficients of chromophores y1–y3 at different densities.

Wt%	r_{33} (pm/V)		
	y1	y2	y3
10	32	34	41
15	61	68	79
20	120	117	128
25	149	138	157
30	–	112	145

^a r_{33} values were measured at the wavelength of 1310 nm.

derived from these chromophores, a series of guest–host polymers were prepared by formulating the chromophores into amorphous polycarbonate (APC) using dibromomethane as solvent. The resulting solutions were filtered through a 0.2 μm PTFE filter and spin-coated onto indium tin oxide (ITO) glass substrates. Films of doped polymers were baked in a vacuum oven at 80 $^{\circ}\text{C}$ overnight to ensure the removal of the residual solvent. The corona poling process was carried out at a temperature of 10 $^{\circ}\text{C}$ above the glass transition temperature (T_g) of the polymer. The r_{33} values were measured using the Teng–Man simple reflection technique at the wavelength of 1310 nm using a carefully selected thin ITO electrode with low reflectivity and good transparency in order to minimize the contribution from the multiple reflections [36].

The r_{33} values of films containing chromophores y1 (film-A), y2 (film-B), y3 (film-C) were measured in different loading densities, as shown in Table 3 and Fig. 5. For chromophore y1, the r_{33} values were gradually improved from 32 pm V^{-1} (10 wt%) to 149 pm V^{-1} (25 wt%), as the concentration of chromophores increased, the similar trend of enhancement was also observed for chromophore y2, whose r_{33} values increased from 34 pm V^{-1} (10 wt%) to 138 pm V^{-1} (25 wt%). Chromophore y3 gained the r_{33} value from 41 pm V^{-1} (10 wt%) to 157 pm V^{-1} (25 wt%).

As reported earlier [37–41], the introduction of some isolation groups into the chromophore moieties to further control the shape of the chromophore could be an efficient approach to minimize interactions between the chromophores, but the isolation group should be suitable. So by introducing the isolation groups into the π -bridge, it controls the shape of the chromophore and decreased the interaction between the chromophore thus can increase the r_{33} value. As Fig. 6 (the optimized structure) shows, the one of the donor benzene rings and the substituted group are on both sides of the conjugated plane, which effectively protected the π -conjugated

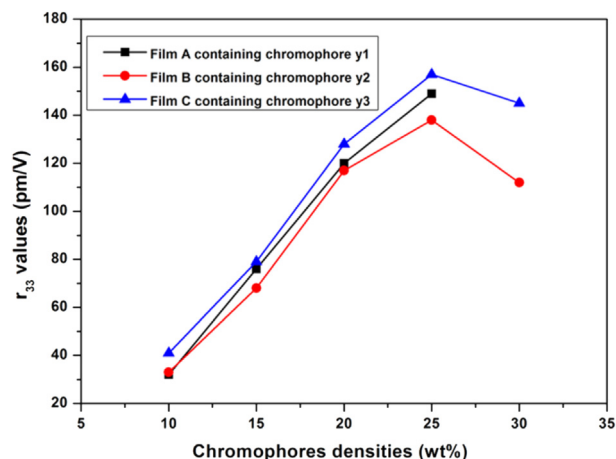


Fig. 5. EO coefficients of NLO thin films as a function of chromophore loading densities.

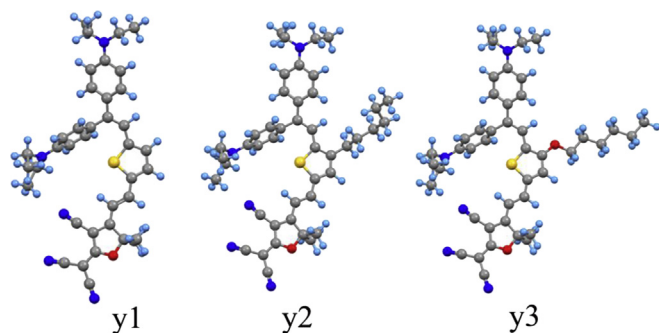


Fig. 6. Optimized structures of chromophores y1–y3.

bridge from an intermolecular Diels–Alder (DA) cycloaddition reaction [42–44]. This arrangement acts to site-isolate the chromophore within the internal free volume created by the substituted group on the thiophene ring, which is favourable for dipole orientation in the poling process. The molecular conformation, including the hindrance of donor and π -bridge (Fig. 6) effectively isolates the chromophores and weakens the dipole–dipole interactions.

The EO coefficient (r_{33}), defining the efficiency of translating molecular microscopic hyperpolarizability into macroscopic EO activities, was described as follows:

$$r_{33} = 2N f(\omega)\beta \langle \cos^3\theta \rangle / n^4$$

where r_{33} is the EO coefficient of the poled polymer, N represents the aligned chromophore number density and $f(\omega)$ denotes the Lorentz–Onsager local field factors. The term $\langle \cos^3\theta \rangle$ is the orientationally averaged acentric order parameter characterizing the degree of noncentrosymmetric alignment of the chromophore in the material and n represents the refractive index [5]. Before poling, there is no EO activity in the EO material and the chromophores in material are thermal randomization. Electrical field induced poling was proceeded to induce the acentric ordering of chromophores. Realization of large electro-optic activity for dipolar organic chromophore-containing materials requires the simultaneous optimization of chromophore first hyperpolarizability (β), acentric order $\langle \cos^3\theta \rangle$, and number density (N). But chromophores with large $\mu\beta$ generate intermolecular static electric field dipole–dipole interaction, which leads to the unfavourable antiparallel packing of chromophores, so that the number of truly oriented chromophore (N) is small. As a result, the isolation groups should be appropriate.

Based on the above view, it is not hard to explain the r_{33} results. When the concentration of chromophore in APC is low, the intermolecular dipolar interactions are relatively weak and thus the influence of different isolation group on r_{33} value is small. As the chromophore loading increased, the effect of inter-chromophore dipole–dipole is becoming stronger. As shown in Table 4, although the resulting r_{33} value of chromophore y2 was 138 pm/V, which was a little smaller than chromophore y1. When effectively normalizes the r_{33} value for the relative chromophore content, dividing the observed r_{33} by N yields a value of 6.39×10^{-19} pm cc/(V molecules), which is larger than chromophore y1 (6.07×10^{-19} pm cc/(V molecules)). Besides, chromophore y3 presented the largest r_{33} values. Hence, film C containing chromophore y2 showed much higher efficiency of translating molecular microscopic hyperpolarizability into macroscopic EO activities. Besides, to our regret, as the loading density increasing from 25 wt% to 30 wt%, the film-A with the loading 30 wt% of y1 showed an

Table 4
Representative r_{33} values of the chromophores.

Chromophores	y1	y2	y3
r_{33} (pm/V) ^a	149	138	157
N ^b	2.455	2.160	2.11
r_{33}/N ^c	6.07	6.39	7.44

^a Experimental value from simple reflection at 1310 nm.

^b Chromophore number density; in units of $\times 10^{20}$ molecules/cc.

^c r_{33} normalized by chromophore number density; in units of $\times 10^{-19}$ pm cc/(V molecules).

obvious phase separation, the film-B and film-C showed a downward trend. The enhancement of the EO activity further demonstrated that the substituted group on thiophene ring effectively suppressed the dipole–dipole interaction and assisted the orientation of chromophores during poling process also improved the compatibility with the polymer. These large r_{33} values and high stability together with our previous work of double donors chromophores can effectively prove that the double donor structure can really decrease the interactions between the chromophores thus can increase the r_{33} values.

4. Conclusions

In this research, two novel chromophores y2 and y3 were designed and synthesized through modification of y1 which we reported previously. These chromophores were systematically characterized by MS, NMR and UV–Vis absorption spectra. The energy gap between ground state and excited state together with molecular nonlinearity were studied by UV–vis absorption spectroscopy, DFT calculations and CV measurements. Theoretical and experimental investigations suggest that the isolation group play a critical role in affecting the linear and nonlinear properties of dipolar chromophores. EO polymers were prepared by the chromophores being doped into APC and their r_{33} values were measured. The poling results of guest–host EO polymers with 25 wt % of these chromophores showed that polymers with chromophores y1–y3 afforded the large r_{33} values of 149, 138 and 157 pm/V respectively. The r_{33} values of EO polymers based on y3 were larger than y1 and y2 due to the alkoxoy chains on the thiophene bridge can not only act as the additional donor group but also an isolation group. Those consequences indicate that these chromophores with double *N,N*-diethylaniline donors and isolation group on the thiophene bridge could efficiently reduce the inter-chromophore electrostatic interactions and enhance the macroscopic optical nonlinearity. All these might be useful in designing other new NLO chromophores with the modified thiophene bridge to optimize the molecular structure for achieving excellent properties. We believe that these novel chromophores can be used in exploring high-performance organic EO and photorefractive materials where both thermal stability and optical nonlinearity are of equal importance.

Acknowledgements

We are grateful to the National Nature Science Foundation of China (no. 61101054) for financial support.

References

- [1] Luo J, Cheng Y-J, Kim T-D, Hau S, Jang S-H, Shi Z, et al. Facile synthesis of highly efficient phenyltetraene-based nonlinear optical chromophores for electro-optics. *Org Lett* 2006;8:1387–90.
- [2] Shi YQ, Zhang C, Zhang H, Bechtel JH, Dalton LR, Robinson BH, et al. Low (sub-1-volt) halfwave voltage polymeric electro-optic modulators achieved by controlling chromophore shape. *Science* 2000;288:119–22.

- [3] Kim S-K, Hung Y-C, Seo B-J, Geary K, Yuan W, Bortnik B, et al. Side-chain electro-optic polymer modulator with wide thermal stability ranging from -46 °C to 95 °C for fiber-optic gyroscope applications. *Appl Phys Lett* 2005;87:061112.
- [4] Dalton LR, Sullivan PA, Bale DH. Electric field poled organic electro-optic materials: state of the art and future prospects. *Chem Rev* 2010;110:25–55.
- [5] Dalton LR, Lao D, Olbricht BC, Benight S, Bale DH, Davies JA, et al. Theory-inspired development of new nonlinear optical materials and their integration into silicon photonic circuits and devices. *Opt Mater* 2010;32:658–68.
- [6] Sullivan PA, Dalton LR. Theory-inspired development of organic electro-optic materials. *Acc Chem Res* 2010;43:10–8.
- [7] Marder SR, Kippelen B, Jen AKY, Peyghambarian N. Design and synthesis of chromophores and polymers for electro-optic and photorefractive applications. *Nature* 1997;388:845–51.
- [8] He MQ, Leslie TM, Sinicropi JA, Garner SM, Reed LD. Synthesis of chromophores with extremely high electro-optic activities. 2. Isophorone- and combined isophorone-thiophene-based chromophores. *Chem Mater* 2002;14:4669–75.
- [9] Dalton L, Benight S. Theory-guided design of organic electro-optic materials and devices. *Polymers* 2011;3:1325–51.
- [10] Ma H, Liu S, Luo JD, Suresh S, Liu L, Kang SH, et al. Highly efficient and thermally stable electro-optical dendrimers for photonics. *Adv Funct Mater* 2002;12:565–74.
- [11] Luo JD, Haller M, Li HX, Kim TD, Jen AKY. Highly efficient and thermally stable electro-optic polymer from a smartly controlled crosslinking process. *Adv Mater* 2003;15:1635–40.
- [12] Luo JD, Liu S, Haller M, Liu L, Ma H, Jen AKY. Design, synthesis, and properties of highly efficient side-chain dendronized nonlinear optical polymers for electro-optics. *Adv Mater* 2002;14:1763–70.
- [13] Zhang X, Aoki I, Piao X, Inoue S, Tazawa H, Yokoyama S, et al. Effect of modified donor units on molecular hyperpolarizability of thienyl-vinylene nonlinear optical chromophores. *Tetrahedron Lett* 2010;51:5873–6.
- [14] Dalton LR. Theory-inspired development of organic electro-optic materials. *Thin Solid Films* 2009;518:428–31.
- [15] Andreu R, Blesa MJ, Carrasquer L, Garín J, Orduna J, Villacampa B, et al. Tuning first molecular hyperpolarizabilities through the use of proaromatic spacers. *J Am Chem Soc* 2005;127:8835–45.
- [16] Zhou X-H, Luo J, Davies JA, Huang S, Jen AKY. Push-pull tetraene chromophores derived from dialkylaminophenyl, tetrahydroquinolyl and julolidinyl moieties: optimization of second-order optical nonlinearity by fine-tuning the strength of electron-donating groups. *J Mater Chem* 2012;22:16390–8.
- [17] Cheng YJ, Luo JD, Hau S, Bale DH, Kim TD, Shi ZW, et al. Large electro-optic activity and enhanced thermal stability from diarylaminophenyl-containing high-beta nonlinear optical chromophores. *Chem Mater* 2007;19:1154–63.
- [18] Wu J, Peng C, Xiao H, Bo S, Qiu L, Zhen Z, et al. Donor modification of nonlinear optical chromophores: synthesis, characterization, and fine-tuning of chromophores' mobility and steric hindrance to achieve ultra large electro-optic coefficients in guest–host electro-optic materials. *Dyes Pigments* 2014;104:15–23.
- [19] Wang L, Liu JL, Bo SH, Zhen Z, Liu XH. Synthesis of novel nonlinear optical chromophore containing bis(trifluoromethyl) benzene as an isolated group. *Mater Lett* 2012;80:84–6.
- [20] Kim TD, Kang JW, Luo JD, Jang SH, Ka JW, Tucker N, et al. Ultralarge and thermally stable electro-optic activities from supramolecular self-assembled molecular glasses. *J Am Chem Soc* 2007;129:488–9.
- [21] Sullivan PA, Akelaitis AJP, Lee SK, McGrew G, Lee SK, Choi DH, et al. Novel dendritic chromophores for electro-optics: influence of binding mode and attachment flexibility on electro-optic behavior. *Chem Mater* 2006;18:344–51.
- [22] Yang Y, Wang H, Liu F, Yang D, Bo S, Qiu L, et al. The synthesis of new double-donor chromophores with excellent electro-optic activity by introducing modified bridges. *PCCP* 2015;17:5776–84.
- [23] Wu W, Wang C, Tang R, Fu Y, Ye C, Qin J, et al. Second-order nonlinear optical dendrimers containing different types of isolation groups: convenient synthesis through powerful “click chemistry” and large NLO effects. *J Mater Chem C* 2013;1:717–28.
- [24] Yang Y, Xu H, Liu F, Wang H, Deng G, Si P, et al. Synthesis and optical nonlinear property of Y-type chromophores based on double-donor structures with excellent electro-optic activity. *J Mater Chem C* 2014;2:5124–32.
- [25] He MQ, Leslie TM, Sinicropi JA. Alpha-Hydroxy ketone precursors leading to a novel class of electro-optic acceptors. *Chem Mater* 2002;14:2393–400.
- [26] Guo X, Watson MD. Conjugated polymers from naphthalene bisimide. *Org Lett* 2008;10:5333–6.
- [27] Zheng S, Barlow S, Parker TC, Marder SR. A convenient method for the synthesis of electron-rich phosphonates. *Tetrahedron Lett* 2003;44:7989–92.
- [28] Dickson RM, Becke AD. Basis-set-free local density-functional calculations of geometries of polyatomic-molecules. *J Chem Phys* 1993;99:3898–905.
- [29] Frisch M, Trucks G, Schlegel H, Scuseria G, Robb M, Cheeseman J, et al. Gaussian 03, revision B. 03. Pittsburgh, PA: Gaussian Inc; 2003.
- [30] Lee C, Parr RG. Exchange–correlation functional for atoms and molecules. *Phys Rev A* 1990;42:193–200.
- [31] Ma X, Ma F, Zhao Z, Song N, Zhang J. Toward highly efficient NLO chromophores: synthesis and properties of heterocycle-based electronically gradient dipolar NLO chromophores. *J Mater Chem* 2010;20:2369.
- [32] Solomon RV, Veerapandian P, Vedha SA, Venuvanalingam P. Tuning nonlinear optical and optoelectronic properties of vinyl coupled triazene chromophores: a density functional theory and time-dependent density functional theory investigation. *J Phys Chem A* 2012;116:4667–77.
- [33] El-Shishtawy RM, Borbone F, Al-Amshany ZM, Tuzi A, Barsella A, Asiri AM, et al. Thiazole azo dyes with lateral donor branch: synthesis, structure and second order NLO properties. *Dyes Pigments* 2013;96:45–51.
- [34] Wu JY, Liu JL, Zhou TT, Bo SH, Qiu L, Zhen Z, et al. Enhanced electro-optic coefficient ($r(33)$) in nonlinear optical chromospheres with novel donor structure. *RSC Adv* 2012;2:1416–23.
- [35] Thanthiruwatte KS, de Silva KMN. Non-linear optical properties of novel fluorenyl derivatives – ab initio quantum chemical calculations. *J Mol Struct Theochem* 2002;617:169–75.
- [36] Teng CC, Man HT. Simple reflection technique for measuring the electro-optic coefficient of poled polymers. *Appl Phys Lett* 1990;56:1734.
- [37] Wu WB, Qin JG, Li Z. New design strategies for second-order nonlinear optical polymers and dendrimers. *Polymer* 2013;54:4351–82.
- [38] Li Za, Li Z, Di Ca, Zhu Z, Li Q, Zeng Q, et al. Structural control of the side-chain chromophores to achieve highly efficient nonlinear optical polyurethanes. *Macromolecules* 2006;39:6951–61.
- [39] Li Z, Li QQ, Qin JG. Some new design strategies for second-order nonlinear optical polymers and dendrimers. *Polym Chem* 2011;2:2723–40.
- [40] Li Za, Wu W, Li Q, Yu G, Xiao L, Liu Y, et al. High-generation second-order nonlinear optical (NLO) dendrimers: convenient synthesis by click chemistry and the increasing trend of NLO effects. *Angew Chem Int Ed* 2010;49:2763–7.
- [41] Wu W, Tang R, Li Q, Li Z. Functional hyperbranched polymers with advanced optical, electrical and magnetic properties. *Chem Soc Rev* 2015;44:3997–4022.
- [42] Hammond SR, Sinness J, Dubbury S, Firestone KA, Benedict JB, Wawrzak Z, et al. Molecular engineering of nanoscale order in organic electro-optic glasses. *J Mater Chem* 2012;22:6752.
- [43] Shi Z, Luo J, Huang S, Zhou X-H, Kim T-D, Cheng Y-J, et al. Reinforced site isolation leading to remarkable thermal stability and high electrooptic activities in cross-linked nonlinear optical dendrimers. *Chem Mater* 2008;20:6372–7.
- [44] Wu J, Bo S, Liu J, Zhou T, Xiao H, Qiu L, et al. Synthesis of novel nonlinear optical chromophore to achieve ultrahigh electro-optic activity. *Chem Commun (Camb)* 2012;48:9637–9.